Journal of Marine Science and Application (2019) 18:334–342
https://doi.org/10.1007/s11804-019-00086-6

RESEARCH ARTICLE

Fast Extraction of Local Underwater Terrain Features for Underwater Terrain-Aided Navigation

Pengyun Chen[1] · Pengfei Zhang[1] · Jianlong Chang[1] · Peng Shen[2]

Received: 24 November 2017 / Accepted: 13 April 2018 / Published online: 21 March 2019

Abstract
Terrain matching accuracy and real-time performance are affected by local underwater terrain features and structure of matching surface. To solve the extraction problem of local terrain features for underwater terrain-aided navigation (UTAN), real-time data model and selection method of beams are proposed. Then, an improved structure of terrain storage is constructed, and a fast interpolation strategy based on index is proposed, which can greatly improve the terrain interpolation–reconstruction speed. Finally, for the influences of tide, an elimination method of reference depth deviation is proposed, which can reduce the reference depth errors caused by tidal changes. As the simulation test shows, the proposed method can meet the requirements of real-time performance and effectiveness. Furthermore, the extraction time is considerably reduced, which makes the method suitable for the extraction of local terrain features for UTAN.

Keywords Underwater terrain modeling · Beam selection · Mixing resolution · Terrain storage model · Index extraction

1 Introduction

With the increasing demands for long-time, precise long-range underwater navigation capabilities of autonomous underwater vehicles (AUVs) (Su et al. 2013; Carreno et al. 2010), studying underwater terrain-aided navigation (UTAN) in depth as a correction method for the cumulative error of inertial navigation systems (INSs) is necessary (Hagen and Anonsen 2014; Chen et al. 2015; Nygren and Jansson 2004).

Article Highlights
- The proposed DTM storage format and index-based interpolation method can improve the interpolation speed effectively, which is favorable for UTAN.
- With beam mode selection, the number of depth data is reduced significantly, such that the matching speed meets the performance requirements.
- Tide correction can improve the matching accuracy, and the real-time performance is scarcely influenced.

✉ Pengyun Chen
chenpengyun@nuc.edu.cn

[1] College of Mechatronic Engineering, North University of China, Taiyuan 030051, China

[2] National Deep Sea Center, Qingdao 266237, China

The UTAN process aims to collect depth data in matching areas limited by INS, extract the local underwater terrain features, and then identify the matching position in a digital terrain map (DTM) using terrain matching algorithms. The matching result is used to correct the INS cumulative error (Bergman and Ljung 1997). Local underwater terrain consists of two elements: (1) real-time underwater terrain and (2) reference terrain provided by DTM. The depth measuring equipment of AUV can be divided into two categories: acoustic altimeter and multi-beam echo sounder (MBES) (Tian 2007). These categories have the same principles. The acoustic altimeter can obtain point-line terrain information, and the MBES can obtain line-surface terrain information. Using acoustic altimeter, one depth data can be obtained in an acoustic pulse (ping), such that data acquisition time is extremely long and navigation performance is low. Through MBES, hundreds and even thousands of depth data can be obtained in each ping (Eleftherakis et al. 2014; GeoAcoustics 2007). Furthermore, data acquisition time is reduced, which makes MBES suitable for UTAN (Anonsen and Hagen 2010). Extracting and modeling underwater terrain features in matching areas from DTM is called terrain interpolation reconstruction (Meduna et al. 2010); this method is extremely beneficial to matching operations to rapidly and accurately obtain local terrain information. Owing to tidal influence, deviations occur between depth data measured at different times

(Gao et al. 2003), and eliminating the effects of reference depth deviation is a key problem.

Based on an analysis of the characteristics of MBES data, a real-time surface terrain matching model is established by selecting beam combiner modes. Then, a tree structure-based underwater terrain storage and the fast interpolation–extraction model is proposed. In addition, an elimination method for reference depth deviation is created. A simulation test shows that the proposed method meets UTAN requirements.

2 Real-Time Terrain Modeling

2.1 MBES Data Modeling

Hundreds and even thousands of depth data can be obtained in each ping using MBES, where the data acquisition mode is developed from point line to line surface. Figure 1 shows a schematic of underwater terrain measurement with MBES (Carlstrom and Nygren 2005).

As shown in Fig. 1, MBES can obtain a terrain profile formed by depth data. In most instances, terrain features provided by one terrain profile are not enough (Sun et al. 2009). Therefore, matching operations need multiple terrain profiles (generally 4 to 10) along sailing direction, which are used in constructing real-time surface terrain. Based on the AUV coordinate system, all depth data consist of incidence angles of beams and slant distance between footprints and transducers. The depth data model involves a single-ping data model and multi-ping combination model:

The single-ping model is defined as follows:

$$\boldsymbol{H}_{\mathrm{ma}} = [a_1 \;\; a_1 \;\; \cdots \;\; a_n] \tag{1}$$

$$\boldsymbol{H}_{\mathrm{mt}} = [t_1 \quad t_2 \quad \cdots \quad t_n] \tag{2}$$

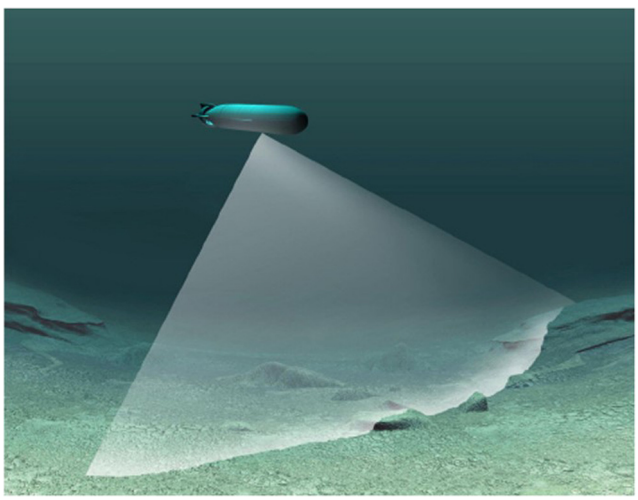

Fig. 1 Real-time measuring using a MBES

In the preceding functions, $\boldsymbol{H}_{\mathrm{ma}}$ is angle matrix, $\boldsymbol{H}_{\mathrm{mt}}$ is slant-distance matrix, a_n is beam incidence angle, and t_n is slant distance.

Similar to the single-ping model, the multi-ping combination model is defined as follows:

$$\boldsymbol{H}_{\mathrm{ma}} = \begin{bmatrix} a_{11} & a_{12} & \cdots & a_{1n} \\ a_{21} & a_{22} & \cdots & a_{2n} \\ \vdots & \vdots & \vdots & \vdots \\ a_{m1} & a_{m2} & \cdots & a_{mn} \end{bmatrix} \tag{3}$$

$$\boldsymbol{H}_{\mathrm{mt}} = \begin{bmatrix} t_{11} & t_{12} & \cdots & t_{1n} \\ t_{21} & t_{22} & \cdots & t_{2n} \\ \vdots & \vdots & \vdots & \vdots \\ t_{m1} & t_{m2} & \cdots & t_{mn} \end{bmatrix} \tag{4}$$

$$\boldsymbol{D}_{\mathrm{mr}} = \begin{bmatrix} (\Delta x_1, \Delta y_1) \\ (\Delta x_2, \Delta y_2) \\ \vdots \\ (\Delta x_m, \Delta y_m) \end{bmatrix} \tag{5}$$

where m is the number of terrain profiles and n is the number of depth data in each terrain profile. The matrix $\boldsymbol{D}_{\mathrm{mr}}$ is called relative-distance matrix. $(\Delta x_i, \Delta y_i)$ is the relative distance between the first terrain profile and ith terrain profile. Thus,

$$\begin{aligned} &\Delta x_1 = 0 \quad \Delta y_1 = 0 \\ &\Delta x_2 = x_2 - x_1 \quad \Delta y_2 = y_2 - y_1 \\ &\Delta x_i = x_i - x_1 \quad \Delta y_i = y_i - y_1 \end{aligned}$$

A large number of depth data can be obtained in one ping using MBES. Thus, the distance measurement error of line-surface terrain is much smaller than that of the point-line terrain obtained by acoustic altimeter, such that the terrain accuracy is high. As the spatial location and depth can be obtained by beam incidence angle and slant distance, the terrain model based on MBES data is presented as follows:

$$\boldsymbol{P}_{\overline{m}} = \begin{bmatrix} t_{11}\sin a_{11} & t_{12}\sin a_{12} & \cdots & t_{1n}\sin a_{1n} \\ t_{21}\sin a_{21} & t_{22}\sin a_{22} & \cdots & t_{2n}\sin a_{2n} \\ \vdots & \vdots & \vdots & \vdots \\ t_{m1}\sin a_{m1} & t_{m2}\sin a_{m2} & \cdots & t_{mn}\sin a_{mn} \end{bmatrix} + \boldsymbol{D}_{\mathrm{mr}} \tag{6}$$

$$\boldsymbol{Z}_{\overline{m}} = \begin{bmatrix} t_{11}\cos a_{11} & t_{12}\cos a_{12} & \cdots & t_{1n}\cos a_{1n} \\ t_{21}\cos a_{21} & t_{22}\cos a_{22} & \cdots & t_{2n}\cos a_{2n} \\ \vdots & \vdots & \vdots & \vdots \\ t_{m1}\cos a_{m1} & t_{m2}\cos a_{m2} & \cdots & t_{mn}\cos a_{mn} \end{bmatrix} \tag{7}$$

where $\boldsymbol{P}_{\overline{m}}$ and $\boldsymbol{Z}_{\overline{m}}$ are the location and depth matrices, which have m terrain profiles.

The description of MBES data is the terrain information from line to surface. Figures 2 and 3 show the line terrain and surface terrain. In Fig. 2, a line terrain is formed by tone terrain profile, and the lateral center distance length is 80 m. Figure 3 shows a surface terrain consisting of 10 terrain profiles, and the distance between adjacent profiles is 10 m.

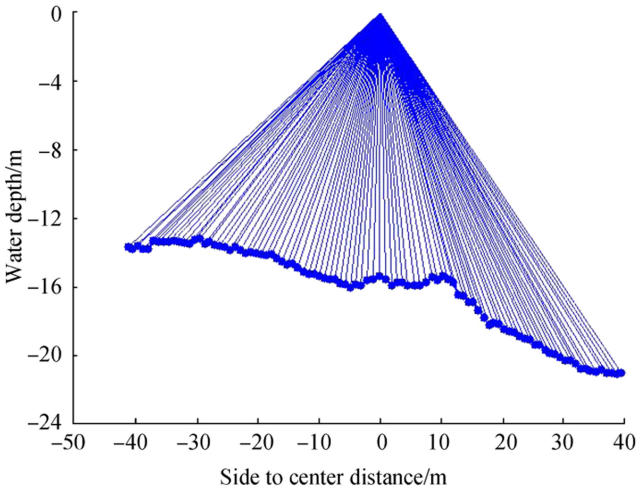

Fig. 2 Line terrain profile of single ping

2.2 Selection Method of Beam Mode

A large amount of depth data can be obtained using MBES. The data amount increases rapidly when multiple terrain profiles are needed. If all data were used for terrain matching, the calculation amount would increase rapidly, thereby seriously affecting the real-time UTAN. With the increase of incidence angle, the accuracy of MBES data is also reduced. Thus, selecting suitable beams is important, which can improve the navigation accuracy. To solve the beam selection problem and considering the characteristics of MBES, a selection method for beam combination mode is proposed in this paper. Based on the beam incidence angle and matching distance, the specific process is as follows:

Condition 1: Beam Incidence Angle

The accuracy and density of MBES data in terrain profile center are low (Zhu and Li 1998) because the center of terrain profile is only at the position of maximum incidence angle. To reduce the influence of depth measurement accuracy, the incidence angle is restricted in $[-\alpha, \alpha]$, and the size of α is determined by data quality. When the approximate depth of navigation area is known, the range of incidence angle can be transformed into the length of side-to-center distance.

Condition 2: Spacing of Side-to-Center Distance

When the range of incidence angle is restricted, a series of depth data with high density can be obtained. If all data were used for matching, the calculation amount would be increased rapidly. Data are selected self-adaptively based on terrain feature function. In other words, the side-to-center distance is considered as a function of terrain profile undulation. By calculating the extent of terrain undulation, we can restrict the distance between the two adjacent beams in the terrain profile, and then the depth data can be selected self-adaptively. Through test selection, the relationship between side-to-center distance with terrain standard deviation σ is expressed as follows:

$$\Delta y = \begin{cases} \mu_1 + \mu_2 \sigma, & \Delta y < d \\ d, & \Delta y \geq d \end{cases} \tag{8}$$

In Eq. (8), Δy is the side-to-center distance in data selection, σ is the terrain standard deviation, μ_1 and μ_2 are the adjustment coefficients determined by grid spacing and measurement accuracy, and d is grid spacing. As shown, Δy is the linear relationship with σ; the larger σ is, the longer is the distance between selected data. However, we have to ensure that more than one depth data is in a grid.

As shown in Fig. 4, the terrain profile has been restricted by beam incidence angle and spacing of the side-to-center distance; the number of original beams is 2889, which is reduced to 43 after beam selection. The beam selection method can

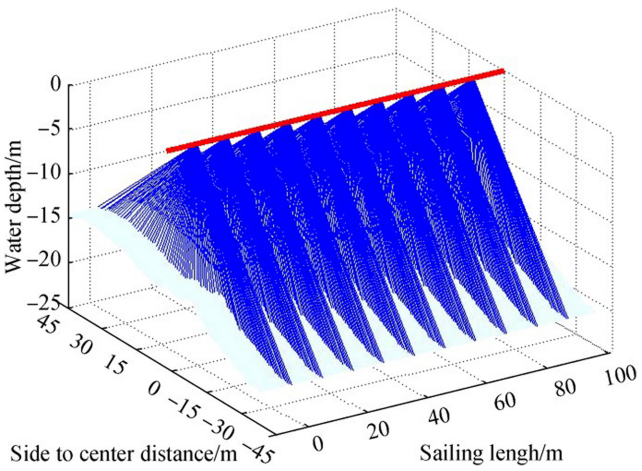

Fig. 3 Surface terrain profiles of 10 pings

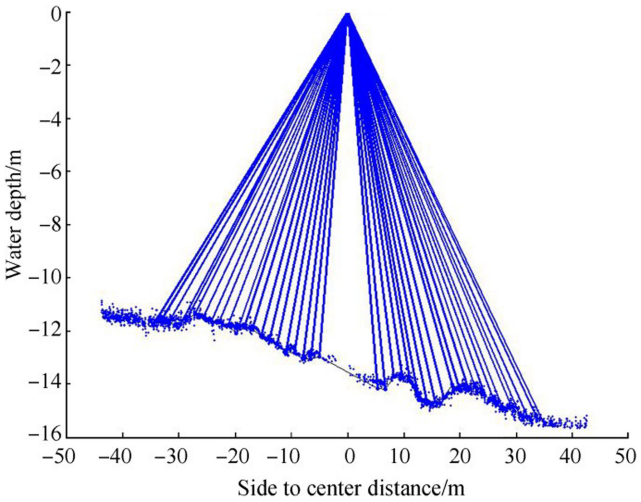

Fig. 4 Selection of depth data

greatly reduce the data amount and the influence of redundant data.

3 Fast Interpolation Method

3.1 DTM Storage Format

Traditional underwater terrain data are sequentially stored in the DTM file according to the order of grid nodes. When the local terrain needs to be extracted and remodeled, the required data are found by loop search. The traversal operation for all terrain data is required every time, which not only is time-consuming but also takes up computer resources greatly, and the real-time performance is affected. Therefore, designing an effective storage model and a fast interpolation–reconstruction method of massive DTM data is significant.

To ensure that the interpolation operation is efficient, a special structure is needed to store the terrain data. Based on the reorganization of original terrain data, a mixing resolution (MR) model is used for terrain data storage. Then, an index-based interpolation–reconstruction strategy is proposed, which can achieve fast terrain interpolation.

The terrain storage model can be divided into hierarchical structure-based (HSB) model and consistent grid model (CGM) (Tan et al. 2003; Wang and Zhu 2012). The tree structure model is the typical representative of the HSB model, which is often used for terrain drawing and image processing (Lu 2003). Owing to the simple structure and high model production efficiency, the quadtree model has been widely used. Through constantly aliquot terrain data, the quadtree model can build the contact between leaf nodes and root nodes recursively, and the terrain modeling and real-time visualization can be achieved. The basic quadtree model is shown in Fig. 5, where each root node can be subdivided into four leaf nodes, and then the terrain detail components can be built gradually.

As shown in Fig. 5, compared with CGM, the HSB model can be classified for every layer, which can compress the search space effectively. However, the HSB model is inconvenient for data operation and has poor search efficiency. To improve the search efficiency, based on the hierarchical idea of quadtree and grid storage mode, an MR storage model is proposed, which aims to restructure and sort terrain data.

The terrain model is based on the following hypothesis: all depth data stored in DTM are true value, the accuracy does not change with grid spacing diversification, and the terrain with under large grid spacing is called low-resolution terrain, and the terrain with under small grid spacing is called high-resolution terrain.

The high-resolution terrain is divided into a combination of low-resolution terrain and high-resolution terrain in MR model. The low-resolution terrain is an explicit feature, and the high-resolution terrain is an implicit feature. As shown in Fig. 6, the nodes marked "□" are the explicit terrain feature nodes, and the nodes marked "●" are the implicit terrain feature nodes.

When storing terrain data, the terrain feature data with different resolutions are stored at the same time, and one tree structure can be composed by an explicit node and a set of implicit nodes, which are stored as a data packet. Among them, the explicit node is a root node and the implicit node is a leaf node. The explicit nodes are stored as CGM and the implicit nodes are stored as a matrix.

The storage form is shown in Fig. 7. In this figure, the file head contains grid size (both explicit and implicit grids) and range of terrain latitude and longitude. The explicit node information contains the index number and depth value, and the implicit node depth value are stored as a matrix. For the fixed storage format, the local terrain information can be easily obtained by the index number and latitude and longitude information. All data are stored as a binary file that can reduce the storage space. For example, a DTM with 1 m × 1 m grid spacing and 5 km × 5 km range contains 25 010 001 depth data. The storage space is approximately 286 MB using traditional

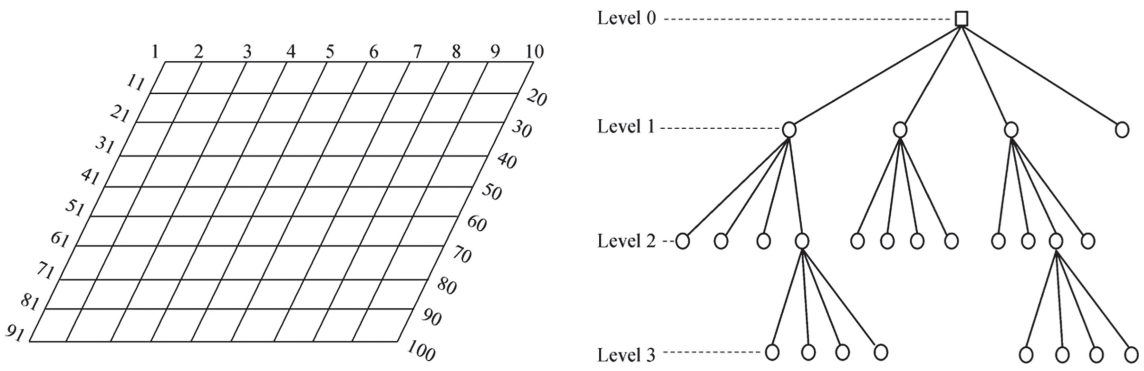

(a) Consistent grid model (b) Quad-tree model

Fig. 5 Storage structure of digital terrain. **a** Consistent grid model. **b** Quadtree model

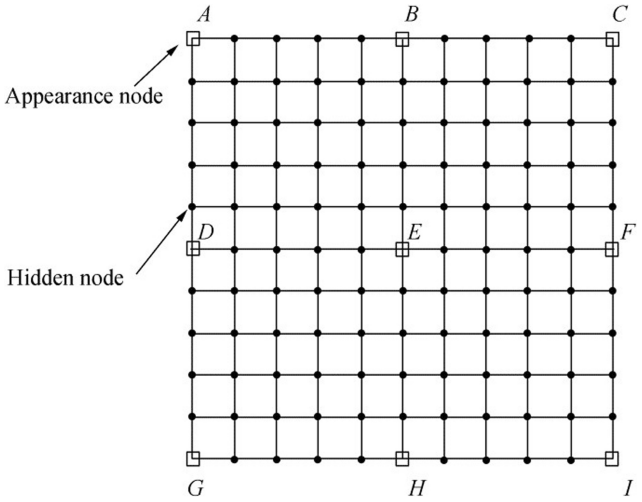

Fig. 6 MR model

storage format and approximately 95 MB using the MR model. If the MR model is used for DTM, the file size is compressed effectively, which is favorable for search and interpolation operation.

3.2 Index-Based Fast Interpolation

The MR-based DTM contains two types of resolution nodes: the explicit nodes are used for fast location and the implicit nodes are used for high-resolution interpolation. The interpolation nodes can be quickly located by index number and then interpolated by implicit node values. We suppose that the latitude and longitude of the interpolated point is (x, y), and the process is divided into two steps.

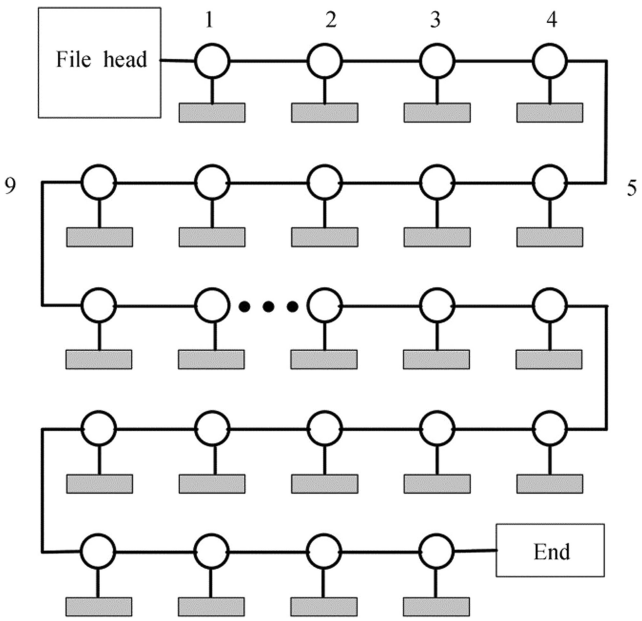

Fig. 7 Storage structure

3.2.1 Local Terrain Block Extraction

According to (x, y) and the range of latitude and longitude, the index numbers of explicit nodes can be calculated. Then, the implicit nodes can be extracted by determining the location of nodes in the DTM file. The calculation functions of index number (I_{xe}, I_{ye}) are as follows:

$$I_{xe} = (x - x_{\min})/d_{xe} + 1 \tag{9}$$

$$I_{ye} = (y - y_{\min})/d_{ye} + 1 \tag{10}$$

In the preceding functions, $x_{\min}$ and $y_{\min}$ are the minimum values of latitude and longitude and d_{xe} and d_{ye} are the grid spacing sizes.

3.2.2 Enlargement of Local Terrain Blocks

To ensure that the local terrain has high resolution, the local terrain needs secondary positioning, which can obtain the implicit index number (I_{xi}, I_{yi}). Then, the high-resolution terrain can be interpolated as follows:

$$I_{xi} = (x - x_e)/d_{xi} + 1 \tag{11}$$

$$I_{yi} = (y - y_e)/d_{yi} + 1 \tag{12}$$

where x_e and y_e are the values of explicit node at (I_{xe}, I_{ye}) and d_{xi} and d_{yi} are the implicit grid spacing sizes.

The interpolation terrain can be restricted to an effective range by the proposed method. Then, the high precise terrain interpolation can be achieved by extracting the high-resolution terrain and releasing the local terrain in this range. Based on the index mechanism, the local terrain can be located fast and reconstruction time is greatly reduced.

3.3 Interpolation Simulation Test

During interpolation simulation, the DTM has 5 km × 5 km range, 10 m × 10 m explicit grid spacing, 1 m × 1 m implicit grid spacing, and approximately 25 million nodes. The computer configurations for the simulation test are an Intel I5 3210 m CPU, 2.5 GHz master frequency, and 8 GB memory. The DTM is stored using CGM and the MR-based model, the searching methods are traversal and index search, and the number of interpolation data is set from 10 to 1000. The results are presented in Fig. 8.

As shown in Fig. 8, using CGM-based DTM and traversal search for interpolation, the time is line increasing with the number of interpolation data increasing. It consumes 2 s with 600 interpolation data, and 3 s with 1000 interpolation data. The computing performance of AUV is much weaker than that of personal computers, so that the interpolation time is longer, which seriously affects the real-time performance of terrain matching. When the MR storage model and index

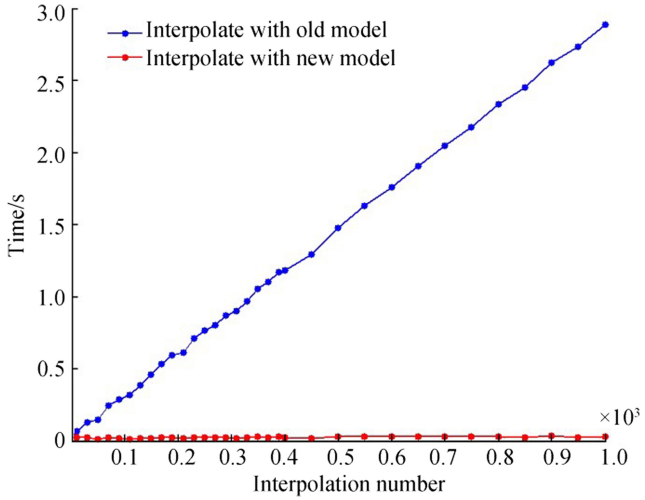

Fig. 8 Time comparison with different model

interpolation are used, the interpolation time is almost unaffected by the number of interpolation data, and the proposed method has good stability. As Fig. 8 shows, the interpolation time is approximately 0.02 s.

4 Eliminating Reference Depth Deviation

In terrain matching using MBES data, reference depth deviation occurs because of the different reference horizontal planes between DTM and real-time depth data affected by tide data. The effect of the reference plane by real-time tide measurement and tide prediction can be reduced, but eliminating it completely is difficult. We suppose that $\{z_t^k\}$ is MBES real-time depth data, $\{h_m^k\}$ is local DTM interpolation data, d_r is the reference horizontal deviation, and the terrain correlation function is as follows:

$$\boldsymbol{T}(\boldsymbol{x}_t) = \sum_{k=1}^{N} \left(z_t^k - h_m^k\right)^2 = \sum_{k=1}^{N} \left(z_t^k - \tilde{h}_m^k + (d_t - d_m)\right)^2 \qquad (13)$$

where $\tilde{z}_t^k$ and $\tilde{h}_m^k$ are terrain data after unified reference plane. Owing to the different reference plane, N is the number of depth data, and the error term $d_t - d_m$ is added into the terrain correlation function. In flat areas, the results are affected and the matching uncertainty is increased. To reduce the effect, based on the mean value method of different colors in image matching processing, the eliminating function of reference depth deviation is as follows:

$$\boldsymbol{T}(\boldsymbol{x}_t) = \sum_{k=1}^{N} \left(z_t^k - h_m^k\right)^2 = \sum_{k=1}^{N} \left(z_t^k - \overline{z}_t - \left(h_m^k - \overline{h}_m\right)\right)^2 \qquad (14)$$

In function (14), $\overline{z}_t$ is the mean value of real-time depth data and $\overline{h}_m$ is the mean value of DTM interpolation data. Figure 9

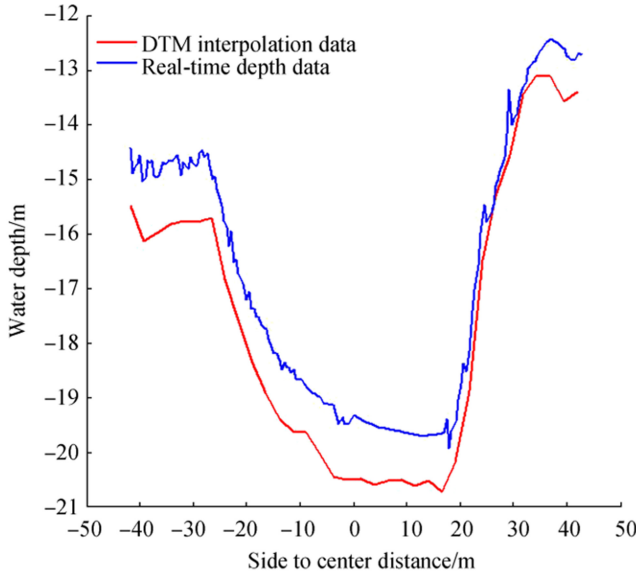

(a) Without depth deviation elimination

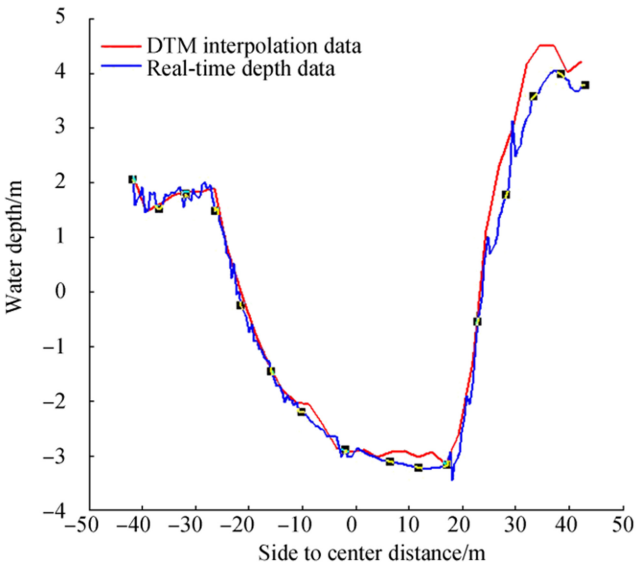

(b) With depth deviation elimination

Fig. 9 Comparison between real-time depth data and local DTM interpolation data. **a** Without depth deviation elimination. **b** With depth deviation elimination.

shows the comparison between real-time depth data and local DTM interpolation data.

5 Simulation and Result Analysis

To verify the proposed method, an underwater terrain area measured by MBES is used for playback simulation, and the maximum likelihood estimation (Peng et al. 2016) is used for the matching algorithm. The matching real-time performance and matching accuracy are compared. The matching

algorithm is the same in simulation, so the main influencing factor is the local underwater terrain features.

The area is 1000 m long, 900 m wide, and 5–40 m deep. The original data are made up of 20 beam lines. After the filtering and gridding process, the following three DTMs are obtained:

DTM-1: terrain storage is based on the MR model, explicit node spacing is 10 m, and implicit node spacing is 1 m;
DTM-2: terrain storage is based on CGM and node spacing is 1; and
DTM-3: terrain storage is based on CGM and node spacing is 5 m.

The path indicated by the arrow in Fig. 10 is an independent multi-beam survey line that is used to simulate real-time sounding data. The survey line is perpendicular to the lines marking the DTM; thus, data independence is ensured. Five matching areas are selected sequentially along the survey line for simulation.

In playback simulation, the real-time measurement of MBES can be simulated by reading the original depth data from the independent survey line, and then the terrain matching simulation can be conducted. As the GPS data in the file of the multi-beam original data are the real-time kinematic data, the theoretical positioning accuracy can reach centimeter level, which can be used for the reference position of terrain. The simulation parameters are shown in Table 1.

The real-time MBES data filtering method is based on the dynamic clustering model. The following five conditions are selected for terrain matching:

1) No beam mode selection, DTM-1 is used, and reference depth deviation is eliminated;

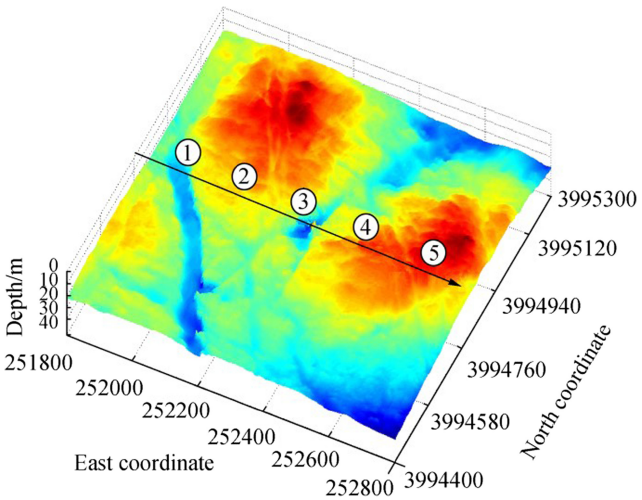

Fig. 10 DTM based on MBES data

Table 1 Simulation parameters

System parameters	Value
Initial error of INS/m	50
Drift error of INS/(km·h^{-1})	1
Speed of AUV/(m·s^{-1})	1
Multi-beam bathymetric error	$N(0, 0.2)$
Other noise errors	$N(0, 0.2)$
Time interval of two adjacent positioning/s	200

2) Beam mode selection, DTM-1 is used, and reference depth deviation is eliminated;
3) Beam mode selection, DTM-1 is used, and reference depth deviation is not eliminated;
4) Beam mode selection, DTM-2 is used, and reference depth deviation is eliminated;
5) Beam mode selection, DTM-3 is used, and reference depth deviation is eliminated.

After filtering, over 3000 depth data are obtained in each terrain profile. A simulation test is conducted under each condition, with the interval distance between two adjacent ping samplings being 20 m after 100 simulation tests. The simulation results are presented in Table 2.

The matching operation by Condition 1 is not completed after 100 s, and the matching fails. The reason is that without beam mode selection, the depth data used for terrain matching are too many, such that the calculated amount is extremely large and the computing power is exceeded. When the results between Conditions 4 and 5 are compared, the terrain matching accuracy is determined by the DTM grid spacing size. By reducing the DTM resolution, the matching time can decrease, but the real-time performance is not high enough with Condition 5. Comparison of Conditions 2 and 4 shows that the matching accuracy is similar, but the matching time of Condition 2 is much less than that of Condition 4. Between Conditions 2 and 3, the matching time of Condition 3 is similar to that of Condition 2, but the matching accuracy is lower. As shown by the terrain matching results in five matching areas, the proposed method enables self-adaptive selection of the beam mode, and the matching accuracy and real-time performance can be ensured.

6 Conclusions

For the extraction of underwater local terrain features for UTAN, we studied the real-time underwater terrain modeling, and then built an MBES-based DTM and interpolation–reconstruction method for UTAN. Finally, a tide correction method was proposed. The following conclusions were reached:

Table 2 Simulation results

Serial number of anchor point		Number of pings	Number of beams	Matching length/m	Average matching time/s	Average matching error/m
1	Condition 1	2	6023	10	> 100	–
	Condition 2	2	159	10	0.13	1.6
	Condition 3	2	159	10	0.12	3.2
	Condition 4	2	159	10	6.22	1.6
	Condition 5	2	159	10	1.19	8.2
2	Condition 1	4	12 031	30	> 100	–
	Condition 2	4	203	30	0.14	1.8
	Condition 3	4	203	30	0.13	3.5
	Condition 4	4	203	30	7.12	1.9
	Condition 5	4	203	30	3.11	9.1
3	Condition 1	2	6019	10	> 100	–
	Condition 2	2	161	10	0.14	1.4
	Condition 3	2	161	10	0.14	3.1
	Condition 4	2	161	10	6.19	1.5
	Condition 5	2	161	10	1.20	8.1
4	Condition 1	3	9221	20	> 100	–
	Condition 2	3	219	20	0.16	2.0
	Condition 3	3	219	20	0.15	3.7
	Condition 4	3	219	20	6.33	1.9
	Condition 5	3	219	20	2.12	8.5
5	Condition 1	5	15 101	40	> 100	–
	Condition 2	5	201	40	0.15	2.0
	Condition 3	5	201	40	0.14	4.0
	Condition 4	5	201	40	6.42	1.9
	Condition 5	5	201	40	1.17	10.2

1) The DTM format affects the matching accuracy and speed, and the matching accuracy is only related by grid spacing size. The proposed DTM storage format and index-based interpolation method can improve the interpolation speed effectively, which is favorable for UTAN.
2) The beam mode selection method is feasible. With beam mode selection, the number of depth data is reduced significantly, such that the matching speed meets the performance requirements.
3) The tide correction can improve the matching accuracy, and the real-time performance is scarcely influenced.
4) Although the file size of DTM has been greatly compressed, the DTM storage space is still extremely high because of the low computer performance of AUV. How to further reduce the DTM size and improve the local terrain extraction speed remains a meaningful research direction.

Funding This study is supported by the National Natural Science Foundation of China (Grant No. 51775518), Natural Science Foundation of North University of China (Grant No. 2017001), and the 333 Academic Start Funding for Talents of North University of China (Grant No. 13011915).

References

Anonsen KB, Hagen OK (2010) An analysis of real-time terrain aided navigation results from HUGIN AUV. Oceans 2010, Seattle, 1–9. https://doi.org/10.1109/OCEANS.2010.5664076

Bergman N, Ljung L (1997) Point-mass filter and Cramer-Rao bound for terrain-aided navigation. IEEE Conference on Decision and Control, San Diego, 565–570. https://doi.org/10.1109/CDC.1997.650690

Carlstrom J, Nygren I (2005). Terrain navigation of the Swedish AUV62f vehicle. 14th International Symposium on Unmanned Untethered Submersible Technology, Durham, 1–10. https://doi.org/10.1109/UUST.2005.5664076

Carreno S, Wilson P, Ridao P, Petillot Y (2010) A survey on terrain based navigation for AUVs. Oceans 2010, Seattle, 1–7. https://doi.org/10.1109/OCEANS.2010.5664372

Chen PY, Li Y, Su YM, Chen XL, Jiang YQ (2015) Underwater terrain positioning method based on least squares estimation for AUV. China Ocean Eng 29(6):859–874. https://doi.org/10.1007/s13344-015-0060-9

Eleftherakis D, Snellen M, Amiri-Simkooei A, Simons DG, Siemes K (2014) Observations regarding coarse sediment classification based on multi-beam echo-sounder's backscatter strength and depth residuals in Dutch rivers. J Acoust Soc Am 135(6):3305–3315. https://doi.org/10.1121/1.4875236

Gao JY, Jin XL, Wu ZY (2003) Construction of submarine DTM from raw multibeam data. Mar Sci Bull 22(1):30–38 (in Chinese). https://doi.org/10.3969/j.issn.1001-6392.2003.01.005

GeoAcoustics Limited (2007) GeoSwath Plus operation manual. GeoAcoustics Limited, London, 1–25

Hagen OK, Anonsen KB (2014) Using terrain navigation to improve marine vessel navigation systems. Mar Technol Soc J 48(2):45–58. https://doi.org/10.4031/MTSJ.48.2.6

Lu YQ (2003) Study of the real-time rendering for large-scale terrain dataset. PhD thesis, Zhejiang University, Hangzhou, 1–6 (in Chinese)

Meduna DK, Rock SM, McEwen RS (2010) Closed-loop terrain relative navigation for AUVs with non-inertial grade navigation sensors. Autonomous Underwater Vehicles (AUV), 2010 IEEE/OES, Monterey, 1-8. https://doi.org/10.1109/AUV.2010.5779659

Nygren I, Jansson M (2004) Terrain navigation for underwater vehicles using the correlator method. IEEE J Ocean Eng 29(3):906–915. https://doi.org/10.1109/JOE.2004.833222

Peng DD, Zhou T, Li HS, Zhang WY (2016) Terrain-aided navigation for underwater vehicles using maximum likelihood method. 2016 IEEE/OES China Ocean Acoustics Symposium, Harbin, 1–6. https://doi.org/10.1109/COA.2016.7535750

Su YM, Zhao JX, Cao J, Zhang G (2013) Dynamics modeling and simulation of autonomous underwater vehicles with appendages. J Mar Sci Appl 12(1):45–51. https://doi.org/10.1007/s11804-013-1169-6

Sun L, Liu YC, Li MS (2009) Technique on building DEM of bathymetry using multibeam data. Hydrographic Surveying and Charting 29(1):39–41 (in Chinese). https://doi.org/10.3969/j.issn.1671-3044.2009.01.012

Tan B, Xu Q, Ma DY (2003) Real-time multi-resolution terrain rendering using restricted quadtree. Journal of Computer-aided Design & Computer Craphics 15(3):270–276 (in Chinese). https://doi.org/10.3321/j.issn:1003-9775.2003.03.005

Tian FM (2007) Research on prior map data processing based terrain-aided navigation methods for underwater vehicles. Master thesis, Harbin Engineering University, Harbin, 10–20 (in Chinese)

Wang YK, Zhu YL (2012) Terrain three-dimensional visualization based on dynamic LOD quadtree arithmetic. IEEE International Conference on Intelligent Control, Automatic Detection and High-End Equipment, Beijing, 1–5. https://doi.org/10.1109/ICADE.2012.6330090

Zhu Q, Li DR (1998) Error analysis and processing of multibeam soundings. Journal of Wuhan Technical University of Surveying and Mapping 23(1):1–4 (in Chinese). https://doi.org/10.3321/j.issn:1671-8860.1998.01.001